Mucus accumulation in the lungs precedes structural changes and infection in children with cystic fibrosis

Charles R. Esther Jr.[1,2*†], Marianne S. Muhlebach[1,2†], Camille Ehre[1,2], David B. Hill[2,3], Matthew C. Wolfgang[2], Mehmet Kesimer[2], Kathryn A. Ramsey[2,4], Matthew R. Markovetz[2], Ian C. Garbarine[2], M. Gregory Forest[5], Ian Seim[5], Bryan Zorn[2], Cameron B. Morrison[2], Martial F. Delion[2], William R. Thelin[6], Diane Villalon[6], Juan R. Sabater[7], Lidija Turkovic[4], Sarath Ranganathan[8], Stephen M. Stick[4,9,10‡], Richard C. Boucher[2‡]

Although destructive airway disease is evident in young children with cystic fibrosis (CF), little is known about the nature of the early CF lung environment triggering the disease. To elucidate early CF pulmonary pathophysiology, we performed mucus, inflammation, metabolomic, and microbiome analyses on bronchoalveolar lavage fluid (BALF) from 46 preschool children with CF enrolled in the Australian Respiratory Early Surveillance Team for Cystic Fibrosis (AREST CF) program and 16 non-CF disease controls. Total airway mucins were elevated in CF compared to non-CF BALF irrespective of infection, and higher densities of mucus flakes containing mucin 5B and mucin 5AC were observed in samples from CF patients. Total mucins and mucus flakes correlated with inflammation, hypoxia, and oxidative stress. Many CF BALFs appeared sterile by culture and molecular analyses, whereas other samples exhibiting bacterial taxa associated with the oral cavity. Children without computed tomography–defined structural lung disease exhibited elevated BALF mucus flakes and neutrophils, but little/no bacterial infection. Although CF mucus flakes appeared "permanent" because they did not dissolve in dilute BALF matrix, they could be solubilized by a previously unidentified reducing agent (P2062), but not *N*-acetylcysteine or deoxyribonuclease. These findings indicate that early CF lung disease is characterized by an increased mucus burden and inflammatory markers without infection or structural lung disease and suggest that mucolytic and anti-inflammatory agents should be explored as preventive therapy.

INTRODUCTION

Abnormal host-environmental interactions in the cystic fibrosis (CF) lung lead to progressive airway destruction, bronchiectasis, and premature death (*1*). The hallmark features of CF lung disease include abnormal mucus, inflammation, and infection (*1*). CF lungs are histologically normal at birth (*1*), but lung disease begins early in life with bronchiectatic airways detectable by 1 year in some children with CF (*2*, *3*). Thus, there is a need to elucidate the pathogenesis of early CF disease to prevent irreversible airways damage.

Abnormal mucus production in the lungs has been postulated to contribute to the early pathogenesis of CF (*4*), as reflected in the early use of the term "mucoviscidosis" to define the syndrome (*5*). Recent studies suggest that abnormal CF transmembrane conductance regulator (CFTR)–mediated ion transport produces dehydrated (hyperconcentrated) airway mucus that adheres to airway surfaces (*6*, *7*), and data from animal models suggest that hyperconcentrated mucus with increased airway mucus adhesion is sufficient to initiate CF-like lung disease (*8*). However, other mechanisms have also been proposed to dominate early CF disease pathogenesis. These mechanisms focus on bacterial infection as an initiating mechanism and include inactivation of antibacterial peptides by high salt or low pH (*9*, *10*), failure to secrete antimicrobial factors from glands (*11*), abnormalities in phagocyte function (*12*), and failure to secrete bicarbonate or thiocyanate (*13*).

The mechanisms that initiate lung disease in CF have been difficult to identify because studying young subjects with CF is challenging, and CF animal models often fail to recapitulate aspects of human CF disease and yield disparate findings (*14*–*16*).

In this study, we used bronchoalveolar lavage fluid (BALF) and chest computed tomography (CT) images from clinically stable infants and preschool children with CF who enrolled in the Australian Respiratory Early Surveillance Team for Cystic Fibrosis (AREST CF) program (*2*, *3*) and compared the data to age-matched control subjects with active pulmonary disease. We analyzed the relationships between airway mucus, inflammation, and bacterial culture/microbiome and tested therapeutic approaches in animal models.

[1]Division of Pediatric Pulmonology, University of North Carolina at Chapel Hill, Chapel Hill, NC 27599, USA. [2]Marsico Lung Institute, University of North Carolina at Chapel Hill, Chapel Hill, NC 27599, USA. [3]Department of Physics and Astronomy, University of North Carolina at Chapel Hill, Chapel Hill, NC 27599, USA. [4]Telethon Kids Institute, University of Western Australia, Perth 6009, Australia. [5]Departments of Mathematics, Biomedical Engineering, and Applied Physical Sciences, University of North Carolina at Chapel Hill, Chapel Hill, NC 27599, USA. [6]Parion Sciences, Durham, NC 27713, USA. [7]Department of Research, Mount Sinai Medical Center, Miami Beach, FL 33140, USA. [8]Murdoch Children's Research Institute, University of Melbourne, Parkville 3052, Australia. [9]Division of Paediatrics and Child Health, University of Western Australia, Perth 6009, Australia. [10]Princess Margaret Hospital for Children, Perth 6009, Australia.
*Corresponding author. Email: charles_esther@med.unc.edu
†These authors contributed equally to this work.
‡These authors contributed equally to this work as senior authors.

RESULTS

Airway mucins were elevated in children with early CF lung disease

Forty-six children (age, 3.3 ± 1.7 years) with stable CF were studied at 62 study visits (Table 1). At each study visit, BAL was performed in the right middle lobe (RML) and in one of the left lobes (lingula in 58 samples and left lower lobe in 4), providing 124 BALF samples. Chest CT scores for bronchial wall thickening (BWT) and bronchiectasis were available from lavaged lobes in 58 subjects with CF, with BWT present in 65.5% of lobes (76 of 116) and BE in 24.1% (28 of 116). BALF samples were obtained via the same protocol from the RML

and lingula of 16 non-CF disease control subjects, providing 32 samples. The control group was similar in age (3.2 ± 2.0 years) but had active respiratory symptoms. Subjects with CF were on anti-staphylococcal prophylaxis at the time of 29 study visits (bronchoscopy), and antibiotics were prescribed within 3 months of 14 other study visits. Seven disease control subjects received antibiotics within 3 months of bronchoscopy. The disease control group had significantly higher rates of cultured BALF pathogens ($P = 0.004$) and lower neutrophil concentrations ($P < 0.001$) than children with CF (Table 1 and tables S1 and S2).

BALF total mucin concentrations were higher in CF compared to non-CF control samples (Fig. 1A). Total mucin concentrations were also significantly elevated in CF samples stratified by pathogenic infection defined as $\geq 10^3$ organisms/ml in BALF culture ($P = 0.008$) (Fig. 1B). In addition to soluble mucins, insoluble material was identified in BALF (fig. S1, A and B), and scanning electron microscopy (SEM) identified this material as mucus "flakes" in both non-CF and CF samples (Fig. 1, C and D, and fig. S1, C and D). Flakes represented 53 ± 16% of total mucins based on refractometry measures of CF BALF supernatants (soluble mucins) versus pellets (insoluble flakes) after centrifugation (10,000*g* for 20 min, $n = 5$; fig. S1E). Quantitative assessments of flake density and mucin content in designated BALF volumes were performed by immunohistochemistry (IHC). Mucin 5B (MUC5B) and mucin 5AC (MUC5AC) were intermixed in flakes from non-CF and CF samples (Fig. 1, E and F), and small numbers of 4′,6-diamidino-2-phenylindole (DAPI)–stained macrophage nuclei were apparent in the flakes. MUC5B and MUC5AC staining intensities, as well as mucus flake density (number) within BALF samples, were higher in CF compared with non-CF BALF samples (Fig. 1G and table S3), and staining intensities correlated with total mucin concentrations in subjects with CF (fig. S1, F and G). Flakes from non-CF samples typically were composed of mucins organized in a thin, filamentous architecture (Fig. 1E), whereas CF flakes exhibited mucins with a more granular, condensed appearance (Fig. 1F). Image analyses confirmed increased granularity of CF flakes, measured as root mean square (RMS) roughness (Fig. 1H) (*17*).

Table 1. Demographics of AREST CF and non-CF disease control populations. See the Supplementary Materials for definitions of infection and pathogens. *P* values are calculated by Student's *t* test for parametric variables, Mann-Whitney for nonparametric variables, and by χ^2 for discrete variables.

	CF	Non-CF	*P*
Subjects, *n*	46	16	–
Age, years	3.3 ± 1.7	3.2 ± 2.0	0.837
Gender, male (%)	19 (41%)	11 (69%)	0.083
CFTR mutations, F508del homozygous	25 (54%)	–	–
CFTR mutations, residual function	2 (4.3%)	–	–
Study visits, *n* (range per subject)	62 (1–3)	16 (1)	–
BALF samples, *n*	124	32	–
BALF TCC, $\times 10^6$ cells/ml (RML only)	6.7 ± 7.2	1.3 ± 1.0	<0.001
BALF % neutrophils (RML only)	18.6 ± 22.3	4.4 ± 5.1	<0.001
Antibiotic treatment*	43 (69%)	7 (44%)	0.080

*Antibiotics within 3 months of bronchoscopy.

Airway mucins were related to inflammation

We next explored associations between mucins and features of the airway microenvironment that occur in early CF lung disease. Neutrophil counts per ml BALF were higher in CF than non-CF controls (table S1), and total mucin concentrations correlated with neutrophil counts and interleukin-8 (IL-8) in CF BALF (Fig. 2, A and B), but not in non-CF BALF (table S4). DNA concentrations in BALF were higher in CF than non-CF ($P < 0.01$; fig. S1H), ~100-fold lower than mucin concentrations (compared to Fig. 1A), and correlated with total mucin concentrations (Fig. 2C). In CF BALF, total mucin

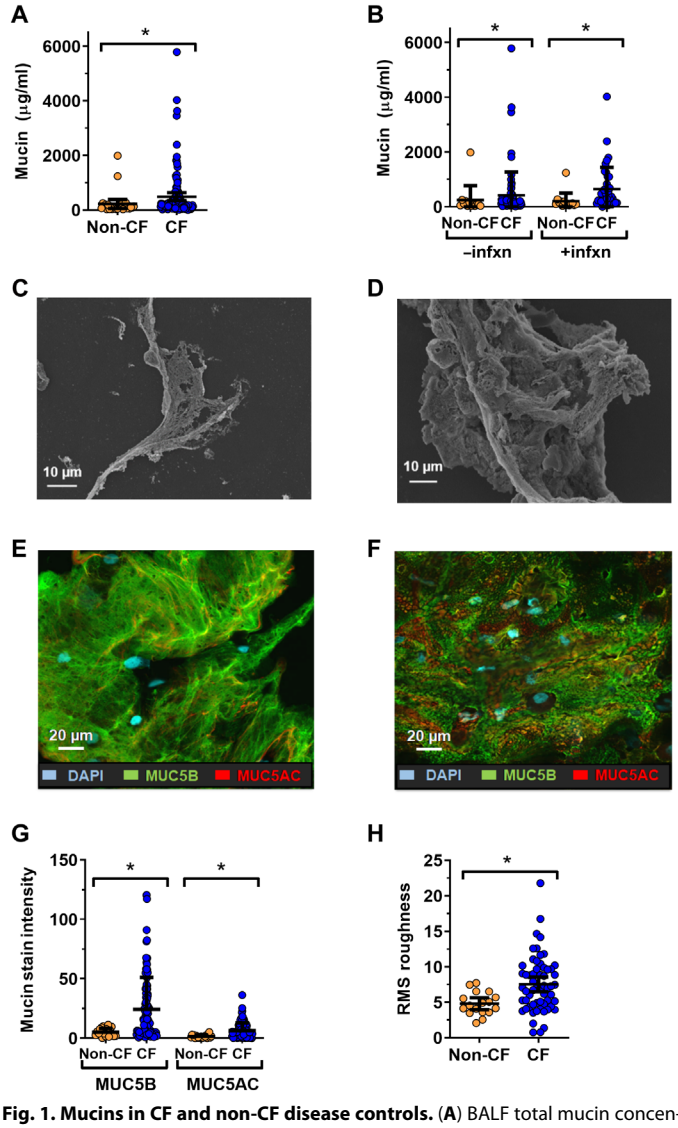

Fig. 1. Mucins in CF and non-CF disease controls. (**A**) BALF total mucin concentrations from subjects with CF ($n = 121$) and non-CF controls ($n = 27$). (**B**) Total concentrations of mucins in BALF after stratification of patients by the absence ($n = 14$ non-CF and 82 CF; left) or presence ($n = 13$ non-CF and 39 CF; right) of pathogenic infection (infxn) on culture of BALF. (**C**) Representative SEM of a flake from a non-CF subject. (**D**) Representative SEM of a flake from a CF subject. (**E** and **F**) Representative IHC of MUC5B (green) and MUC5AC (red) in a cytospin from (E) a non-CF and (F) a CF BALF. (**G**) Mucin staining intensities, an index of flake number, of MUC5B and MUC5AC in CF ($n = 109$) and non-CF ($n = 21$) BALF. (**H**) Flake granularity, measured via image analysis of RMS roughness in CF ($n = 17$) and non-CF ($n = 59$) BALF. *$P < 0.05$; **$P < 0.01$ after multivariate analysis.

concentrations also correlated with metabolomic biomarkers of (i) neutrophilic inflammation (*18*, *19*), including hypoxanthine (Fig. 2D) and other metabolites (table S4); (ii) hypoxia (lactate) (Fig. 2E); and (iii) oxidative stress (oxidized to reduced glutathione ratio) (Fig. 2F). Mucus flake densities also correlated with these inflammatory and metabolomic markers in CF samples (table S4), including after multivariate analysis (table S5).

The CF muco-inflammatory environment was evident without infection

Standard cultures of BALF revealed that in the control group, there was higher incidence and quantity of pathogenic bacteria compared to patients with CF (Fig. 3A). These differences were confirmed when focusing on more pronounced infection [$\geq 10^4$ colony-forming units (CFU)/ml], as used in previous studies (table S2) (*20*). To address the possibility that standard cultures failed to detect relevant bacteria, microbiome analyses were performed, and on the basis of bacterial DNA availability, total bacterial burden was measured by quantitative polymerase chain reaction (qPCR). Sufficient bacterial DNA was available for sequencing and qPCR in 73 and 53% of CF samples and 94 and 88% of non-CF controls, respectively. Availability of bacterial DNA for sequencing did not correlate with mucin concentrations or other factors (fig. S2, A to E).

Mean qPCR values for CF samples were significantly lower than non-CF disease controls, consistent with bacterial culture data (P = 0.001) (Fig. 3, A and B). CF samples with lower qPCR signal (<5000) had a microbiome profile of diverse taxa associated with background (reagent) contamination, similar to washes from sterile bronchoscopes and non-CF samples with lower qPCR signal (Fig. 3C). In contrast, the microbiome samples with higher qPCR values (>5000) were dominated by taxa associated with the oral cavity in both CF and non-CF controls (Fig. 3D and fig. S2, F and G). Although per protocol antibiotic use was common in subjects with CF, it did not appear to alter conventional culture results (fig. S3, A and B), qPCR signals (fig. S3C), or microbiome profiles (Fig. 3C and fig. S3D) in this cohort.

To evaluate the earliest stages of CF lung disease, BALF samples obtained from lobes without substantial CT-defined structural lung disease, classified as "CF–no structural disease" (CF-NSD), were studied (39 samples and 18 subjects; see data file S1). The age at sample collection was similar for CF-NSD samples than subjects with CF with structural disease (table S6), although some infants were not included in this group because they had developed structural lung disease at their first study visit. The CF-NSD samples had an increased density of mucus flakes ($P < 0.05$) and higher neutrophil concentrations ($P < 0.02$) compared with non-CF controls (Fig. 3, D and E, and tables S3 and S6). This CF muco-inflammatory environment was evident despite a low infectious burden measured as (i) a low incidence of culture-defined infection [79 and 92% uninfected at infection definitions (10^3 and 10^4 CFU/ml, respectively); table S6]; (ii) qPCR values lower in the CF-NSD group than the non-CF control group ($P < 0.001$) (Fig. 3F and table S6); and (iii) a CF-NSD microbiome mostly characterized by a reagent-derived texture similar to the sterile bronchoscope wash samples irrespective of antibiotic use (Fig. 3G).

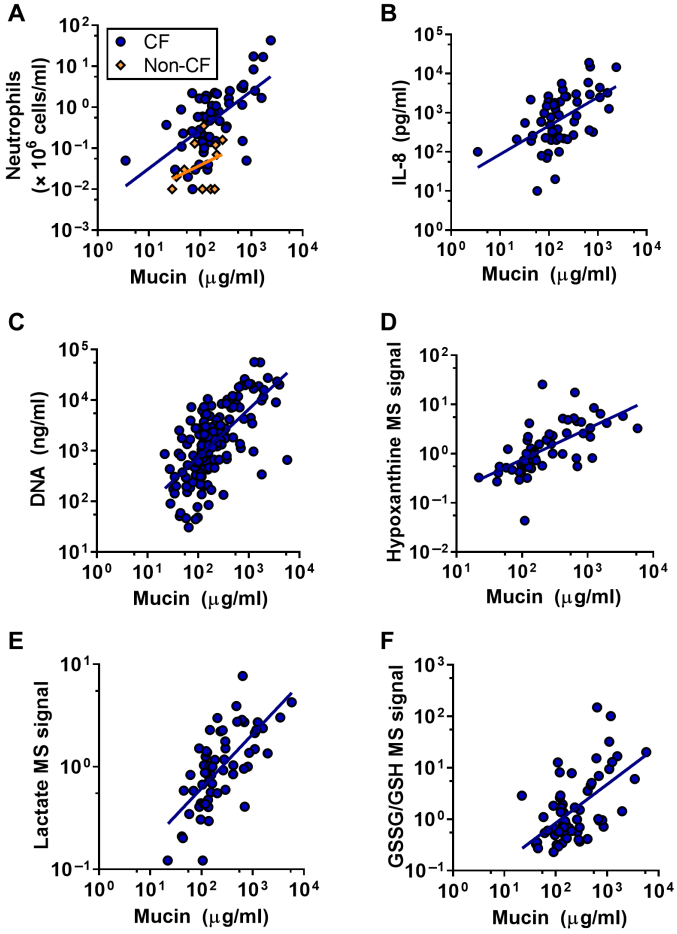

Fig. 2. Mucins and markers of airway disease in early CF. (**A**) Correlation between mucins and neutrophil counts in BALF from subjects with CF (blue; $r^2 = 0.38$, $P < 0.001$, $n = 62$) and non-CF controls (orange; $n = 16$, not significant). (**B** and **C**) Correlations between mucins and other markers associated with neutrophilic inflammation including (B) IL-8 ($r^2 = 0.29$, $P < 0.001$, $n = 62$) and (C) DNA ($r^2 = 0.43$, $P < 0.001$, $n = 62$). (**D** to **F**) Correlations between mucins and BALF metabolite concentrations measured by metabolomics in 60 CF BALF samples, including (D) hypoxanthine ($r^2 = 0.47$, $P < 0.001$) as a marker of inflammation, (E) lactate ($r^2 = 0.48$, $P < 0.001$) as a marker of hypoxia, and (F) ratio of oxidized to reduced glutathione (GSSG/GSH) as a marker of oxidative stress ($r^2 = 0.33$, $P < 0.001$).

Airway mucins in CF were in the form of "permanent" gels

The persistence of mucus flakes in the dilute BALF matrix suggested that flakes were resistant to swelling and dissolution; in other words, were permanent gels (*21*, *22*). To assess therapeutic options to dissolve permanent gels present in BALF from children with CF, the efficacy of prototypic mucolytic agents, including reducing agents [for example, dithiothreitol (DTT)] that break mucin disulfide bonds and deoxyribonuclease (DNase) that cleaves DNA, were studied in CF BALF. DTT, but not DNase, decreased flake numbers as identified by MUC5B or MUC5AC IHC staining intensity (Fig. 4, A and B). The fact that DNA staining appeared to be contained largely to DNA nuclei (Fig. 4A; also see Fig. 1, E and F) explains the absence of DNase activity on DNA staining signal. To address the possibility that reducing agents such as DTT could reduce the intensity of mucin IHC staining due to loss of epitope availability (*6*), reduced flake density and size after DTT treatment were confirmed by SEM (Fig. 4C). Similar effects of DTT were also observed using microrheologic methods to assess mucus flake treatment responses (fig. S4, A and B).

Although DTT proved effective in these experiments using BALF from children with CF, cellular toxicities preclude use of this

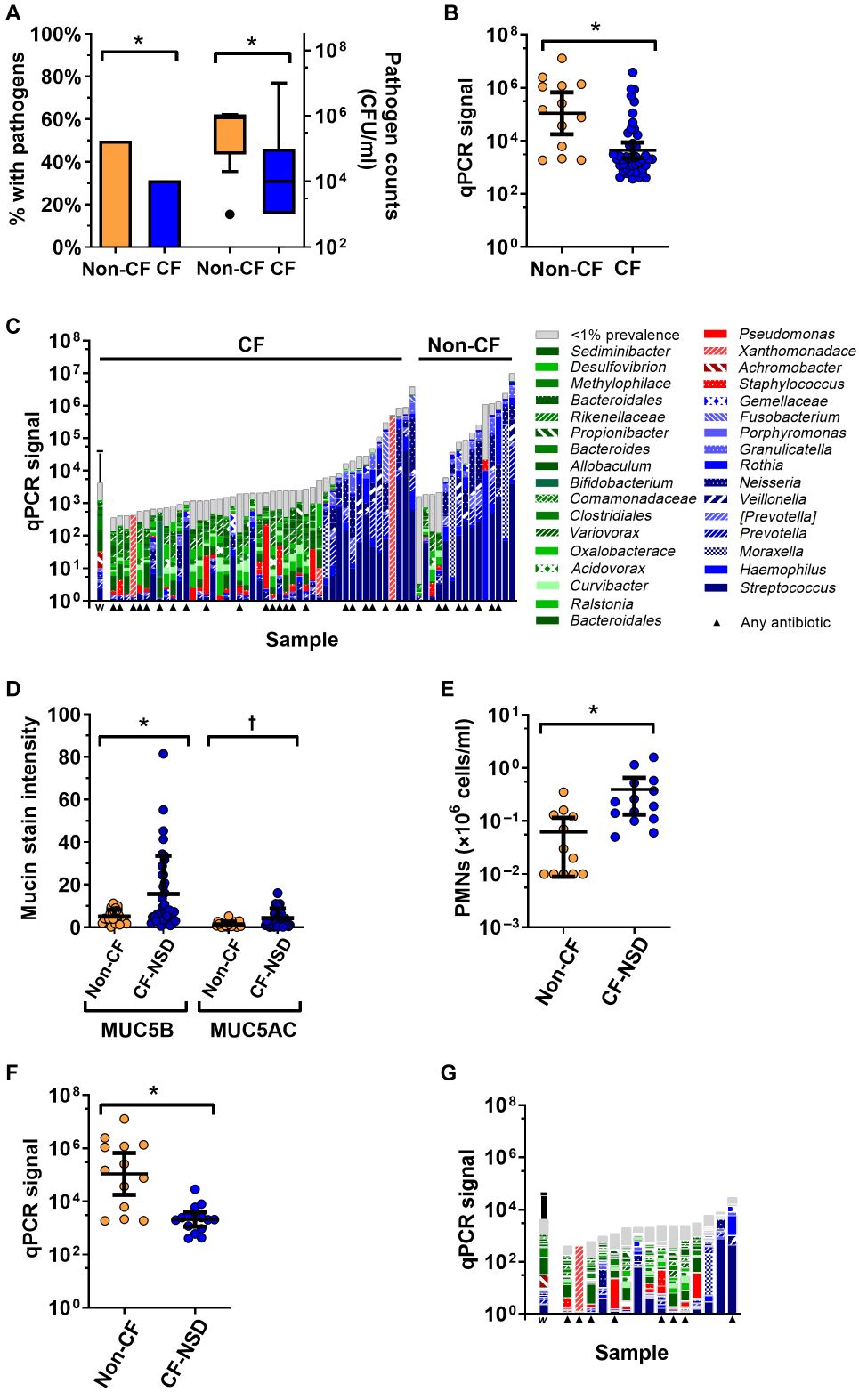

Fig. 3. Bacterial cultures and the microbiome in early CF. (**A**) Pathogen recovery frequency (left) and burden of pathogens in samples with positive cultures (right) in BALF from subjects with CF and from non-CF controls ($n = 124$ CF and 32 non-CF). (**B**) Total bacterial burden, as measured by 16*S* qPCR, in BALF from subjects with CF and non-CF controls ($n = 46$ CF and 15 non-CF). (**C**) qPCR and distribution of taxa from microbiome analyses for all CF (left) and non-CF samples (right). Bar height represents total qPCR signal, with detected taxa represented proportionally within the bar. For clarity, taxa with average prevalence <1% were grouped (light gray bars). The pattern observed from washes of sterile bronchoscopes (*w*) is shown for reference ($n = 6$). Taxa associated with environmental contamination are shown in green; taxa associated with the oral cavity, including *Moraxella*, *Haemophilus*, and *Streptococcus* as common upper airway commensals (*72*), are shown in blue; and known pathogens are shown in red. Taxa were grouped as previously described (*39*). (**D**) Concentrations of MUC5B and MUC5AC as measured by IHC in mucin flakes recovered by BALF from subjects with CF with no structural lung disease (CF-NSD, $n = 37$) and non-CF controls ($n = 21$) (significant by parameter; $P = 0.054$ postmultivariate analyses). (**E**) Neutrophil (PMN) counts in CF-NSD versus non-CF. (**F**) qPCR in CF-NSD and non-CF samples. (**G**) Microbiome analyses of CF-NSD. Triangles represent samples from subjects who received antibiotics ≤3 months before bronchoscopy. See (C) for taxa legend. $^{*}P < 0.05$, $^{\dagger}P < 0.05$ by nonparametric analysis.

compound as a human therapeutic (*23*). The only approved reducing agent for human use, *N*-acetylcysteine (NAC), was tested despite its limited efficacy as an inhaled mucolytic agent (*21*). For comparison, we tested the therapeutic activity of P2062, a novel reducing agent currently in development (fig. S5A). P2062 exhibits more robust reducing activity compared to NAC or DTT in model system assays (fig. S5, B to D) with less evidence of cellular toxicity ($P < 0.05$ P2062 versus DTT at 10 and 100 mM concentrations; fig. S5E). Treatment of mucin flakes with P2062 had effects similar to DTT, with reductions in flake size by SEM (Fig. 4D) and changes in rheology (fig. S5F). In contrast, NAC was ineffective in both assays. To more rapidly measure density of flakes in samples, we developed an imaging method based on image analyses of fluorescent beads embedded in mucus flakes (fig. S5G). Using this method, the density of flakes was found to be decreased significantly by administration of P2062 ($P < 0.05$), but not NAC (Fig. 4E).

To test the impact of aerosolized P2062 in vivo, we used a sheep model in which measurements of tracheal mean velocity (TMV) serve as a marker of mucociliary clearance (*24*). Inhalation of nebulized P2062 (2.5 ml of 50 mM P2062 over 10 min) or saline vehicle

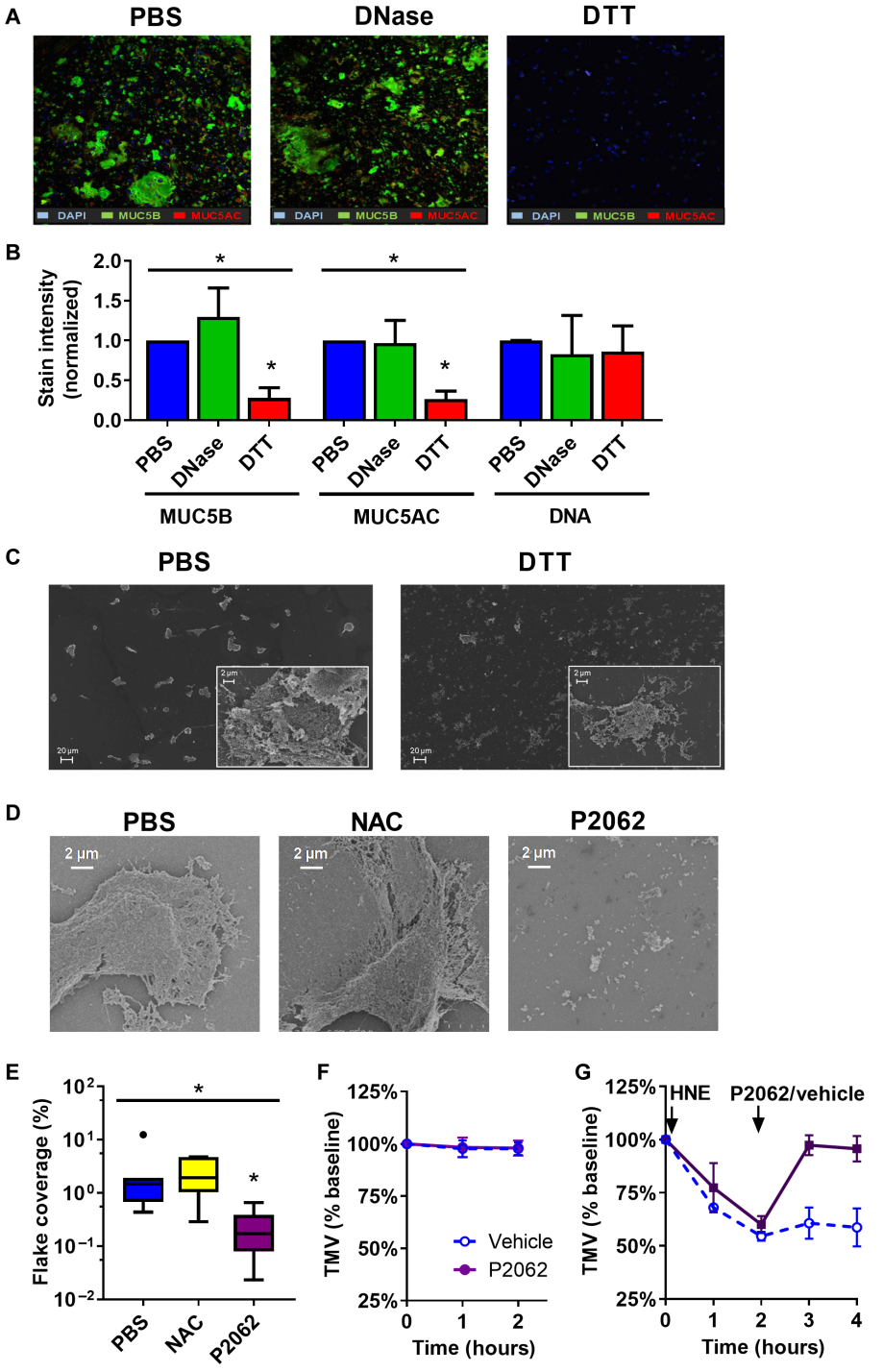

Fig. 4. Treatment of mucin flakes in early CF. (**A**) IHC of MUC5B (green), MUC5AC (red), and DNA (blue) on a cytospin of unprocessed CF BALF treated with (PBS), DNase (300 U/ml), or the reducing agent DTT (10 mM) for 60 min at 37°C. (**B**) Staining intensities of MUC5B and MUC5AC in DTT-treated samples relative to those with vehicle (PBS) or DNase ($n = 5$ per group). Lack of effect of DNase on DNA staining intensities reflected the intracellular location of most DNA. All intensities were normalized to the average values from the PBS group ($n = 10$ per group). (**C**) Flake density in PBS and DTT-treated samples analyzed by SEM. (**D**) Flake density and structure by SEM in samples treated with NAC (10 mM, 1 hour at 37°C) or the novel therapeutic P2062 (10 mM, 1 hour at 37°C). (**E**) Imaging analysis of flake density in CF BALF samples treated with NAC or P2062 ($n = 7$ per group). (**F**) TMV, a measure of mucociliary clearance, in sheep treated with nebulized P2062 (solid purple line; 2.5 ml, 50 mM concentration) or saline (dashed blue line) ($n = 3$ per group). (**G**) TMV in sheep exposed to inhaled neutrophil elastase followed by treatment with nebulized P2062 (solid purple line) or saline (dashed blue line) did not ($n = 3$ per group).

control did not alter baseline TMV (Fig. 4F). Inhalation of human neutrophil elastase (HNE) reduces TMV secondary to increased mucus production (*25*) and airway dehydration (*26*). Treatment with P2062, but not vehicle, rapidly restored TMV to normal values (Fig. 4G).

DISCUSSION

In CF, there is an episodic, heterogeneous failure of airway host defense (*1*, *27*). To characterize the modulation of the host defense components in early CF lung disease and identify prevention strategies, lower airway samples from children with stable CF enrolled in AREST CF were compared to non-CF control children with active/persistent lung disease. This design was necessitated by the obvious inability to bronchoscope healthy infants/children as controls.

Using integrated biochemical and biophysical analyses of BALF samples, a number of observations were made that yielded insights into the nature of early CF lung disease. Our results showed that young children with stable CF airway disease exhibited increased quantities of total mucins compared to non-CF controls. The increase in CF subject BALF mucins occurred despite low infection. Permanent mucus flakes composed of MUC5B and MUC5AC were identified in CF BALF. Although not specific to CF, flakes were greater in number in CF and more closely correlated with neutrophilic inflammation compared with non-CF controls. Moreover, the CF mucus flakes exhibited a distinctive granular appearance compared to controls, consistent with a phase separation that may reflect mucin hyperconcentration (*28*, *29*).

We speculate that the flakes in CF BAL represent mucus plaques "flushed off" CF airway surfaces by the BAL procedure. The interspersion of the superficial epithelium-specific MUC5AC mucin with MUC5B mucin, a product of superficial epithelia and submucosal glands, together with trapped/encased airway macrophages, argues for formation of these flakes by superficial airway epithelia. Mucus flakes appearing to flatten superficial airway cilia have been observed in SEM of small airways in lungs excised from young subjects with CF (*30*). This flake structure contrasts with the long and thick strands of macrophage-free

MUC5B mucin cores secreted from large airway submucosal glands that are coated with threads of MUC5AC secreted by surface epithelia (*31*–*33*). Thus, the mucus flakes observed in our study are distinct from the abnormal submucosal gland mucus strands described in tracheas excised from pig models of CF (*31*, *33*). We cannot exclude a role for abnormal large airway submucosal gland secretion in early CF. However, our observations suggest that the origin of early CF lung disease involves increased quantities of mucins and mucus flakes covering small airway surfaces, findings consistent with the pathological, functional, and imaging data supporting a small airway origin of early CF lung disease (*8*, *9*, *34*).

Our data suggest that bacterial infection is not required for the earliest stages of CF lung disease, suggesting that impaired antimicrobial defenses reflecting possible changes in airway salt, pH, or phagocyte function are not initiating defects in CF (*9*–*13*). Elevated total mucin concentrations and inflammatory markers were observed in children with CF despite a low incidence of pathogens identified by culture or molecular microbiology. This muco-inflammatory state also characterized our CF population with the earliest lung disease (without substantial CT-defined structural changes) in the setting of little or no pathogen infection. These findings are congruent with some, but not all, CF animal models. Recent reports indicate that adult CF ferrets treated continually with an aggressive three-antibiotic regimen manifest a progressive, sterile muco-obstructive bronchiectatic disease (*15*). However, the relative sterility of many early AREST CF BALF samples contrasts with observations in the CF pig model that suggest infection, triggered by pH-dependent inactivation of antibacterial peptides, represents the initiating CF defect that subsequently triggers muco-obstruction (*10*, *35*). Recently, direct measurements of airway pH in children with CF in the AREST CF cohort have not demonstrated the pH changes reported from CF pig models (*36*).

Our data do not diminish the role for bacterial infection in the evolution of CF lung disease. The qPCR and microbiome data suggest that infection can be superimposed on the early CF environment. However, similar to previous reports, the taxa detected were largely related to oral bacteria, not classic CF pathogens (*37*–*39*). Recent data indicate that organisms that contribute to oral bacterial community proliferate well in mucins and low O_2 (*40*, *41*), consistent with the high mucin and lactate concentrations measured in early CF BALF in our study. Thus, we speculate that oral bacteria are aspirated into an environment characterized by mucus accumulation (adherent plaques/flakes) and hypoxia. Once a certain density is achieved, oral flora may be pathogenic (*42*) and can condition anaerobic mucus environments for invasion by classic CF pathogens such as *Pseudomonas aeruginosa* (*43*). Thus, the combination of a hypoxic mucus environment and oral anaerobic bacteria might set the stage for the well-characterized acceleration of CF disease severity associated with acquisition of *Pseudomonas* infection and other pathogens (*20*, *44*).

These findings raise the question of what triggers the muco-inflammatory phenotype in the early CF lung. The heterogeneity of early CF lung disease, mimicking the heterogeneity of early childhood aspiration and viral infections (*45*, *46*), suggests that these insults trigger the early muco-inflammatory phenotype. Viral infections and aspiration both directly stimulate both inflammation (*47*, *48*) and mucin secretion (fig. S6) (*49*). We speculate that under physiological conditions, the effects of virus/aspiration-induced inflammation and mucin secretion are resolved by epithelial hydration and clearance of the inflammatory stimulus, as well as inflammatory cells and newly secreted mucins. The coordination of epithelial mucin secretion and hydration "flush" the airway and allow the resolution process to proceed.

In contrast, we hypothesize that in patients with CF, airways might exhibit a unique defect in the clearance of newly secreted mucins (fig. S6), because the CFTR-dependent epithelial ion transport mechanisms that normally hydrate airway surfaces after inflammatory insults are defective/missing. Thus, mucins secreted in response to insults would be poorly hydrated and form hyperconcentrated mucus masses/plaques that could osmotically compress cilia and adhere to airway surfaces (*8*, *50*). These adherent mucus plaques might provide the nidus/site for a positive feedback cycle between inflammation and mucin secretion (fig. S6). As one component of this cycle, hyperconcentrated, adherent mucus plaques can produce local epithelial hypoxia and trigger inflammatory responses in the absence of pathogens, likely in part mediated by IL-1α (*51*). The relevance of this pathway to early CF lung disease is supported by the observed relationships between mucin, lactate, and neutrophil concentrations in our study and IL-1α release in other AREST CF BAL studies (*52*). As the second component of this cycle, inflammation worsens muco-obstruction by releasing cytokines (including IL-1β and tumor necrosis factor–α), perhaps from airway macrophages, that stimulate mucin secretion (*51*). Consequently, the muco-inflammatory state is perpetuated after removal of the initiating stimulus (*53*, *54*). Note that intrinsic CF-specific hyperinflammation may also contribute to this positive feedback loop (*16*, *55*). This sterile inflammation is only worsened by the bacterial infection that is a feature of later CF lung disease (*20*).

With respect to therapy, our findings suggest that treatments that target mucus accumulation and/or inflammation may be beneficial in early CF. The effectiveness of anti-inflammatory therapies such as ibuprofen (*56*) and azithromycin (*57*) in CF may reflect their impact on this muco-inflammatory milieu, although their modest impact may be overwhelmed with increasingly severe inflammation with age. Newer, more targeted anti-inflammatory agents, including blockers of the IL-1 pathway, may also prove effective in CF lung disease (*58*), although reducing inflammation has the risk of interfering with the ability to prevent/resolve bacterial infection (*59*).

A parallel strategy is to clear accumulated, adherent mucus. Recent studies suggest that formation of adherent mucus plaques/plugs on airway surfaces, rather than just slowing of mucociliary clearance, drives airflow obstruction (*50*). Further, the early anaerobic infection observed in early CF lungs may reflect infection of adherent, anaerobic plaques. Thus, a reasonable therapeutic goal is to clear mucus as a nidus of infection and inflammation from the lung. However, the presence of mucus flakes in early CF disease, as well as their persistence even when diluted in excess solvent, suggests that clearing mucus remains challenging.

Biophysical studies of polymer gels, however, have provided an understanding of mucus flake formation and strategies to clear them. Simple gels, including human bronchial epithelial (HBE) mucus in vitro, are reversible gels that dissolve readily into excess solvent (*60*). In contrast, more complex or modified gels maintain their structure in excess solvent and are permanent, with their properties reflecting long-live bonds between adjacent polymers (mucins) in the gel (*22*). Neither cleavage of DNA nor hydration dissolved the permanent mucus flakes observed in early CF BALs, suggesting that commonly used CF therapies directed toward cleaving DNA or rehydrating mucus may not clear mucus from the lungs of young children with

CF (*61*). In contrast, a reducing agent, DTT, allowed mucus to dissolve with appropriate hydration. This result suggests that DTT may have reduced oxidant-induced S-S intermucin bonds formed during inflammation (*21*). Because the only currently approved reducing agent, NAC, has limited activity against mucus in CF (*21*), including the CF mucus flakes harvested in BALF, development of novel reducing agents will be necessary to test the effectiveness of this class of agents in the clinic. P2062, a reducing agent, dissolved CF BAL flakes in vitro and restored elastase-induced decrements in sheep TMV in vivo, therefore representing a potential mucolytic candidate for treating early CF.

Our study has inherent limitations, including (i) the requirement for bronchoscopy under anesthesia to sample lower airways of children, necessitating lengthy observational intervals and eliminating on ethical grounds a healthy control group; and (ii) per protocol prophylactic/intermittent antibiotic use, rendering it impossible to rule out a role for treated/intermittent bacterial infection in early CF pathogenesis. However, control subjects likely exhibit raised mucin and inflammatory cell values compared to healthy controls (*62*), and antibiotic use did not appear to meaningfully affect the frequency or quantity of bacteria detected by standard cultures or molecular microbiology. These considerations may lessen the impact of these limitations on our conclusion that a muco-inflammatory environment characterizes the early CF lung in the absence of concurrent bacterial infection. Nevertheless, studies of human patients with CF and without early antimicrobial prophylaxis, if available, and studies that noninvasively sample lower airways of CF and healthy subjects will be required to unambiguously assess the role of bacterial pathogens in early CF and absolute differences in CF versus healthy lower airway mucins.

In summary, the earliest stage of CF lung disease is characterized by increased total mucin concentrations and permanent mucus flakes associated with inflammation and airway luminal hypoxia in the absence of routine bacterial infection. Anti-inflammatory agents and agents designed to remove permanent mucus covering airway surfaces of young children with CF appear to be rational strategies to prevent bacterial infection and disease progression, although these approaches likely will require development of novel therapeutics.

MATERIALS AND METHODS

Study design

This was a cross-sectional cohort study comparing measures of mucins, infection, and inflammation in BALF collected from preschool children with CF to BALF collected from age-matched, disease control children. Subjects included (i) children with CF enrolled in AREST CF at the Princess Margaret Hospital for Children (PMHC) in Perth, Australia studied at annual visits from ages 3 months to 6 years (*2*, *3*); and (ii) non-CF disease control preschool children undergoing clinically indicated bronchoscopy at the PMHC for persistent cough, wheeze, or other respiratory symptoms/signs (table S1). All subjects underwent bronchoscopy with BAL from two separate lobes, with lavages divided into aliquots for mucin, metabolomic, and microbiome analyses. For this study, the first lavage sample from each lobe was divided into two aliquots, an unprocessed sample reserved for mucin measures and a second aliquot centrifuged at 3000*g* for 5 min, with the pellet reserved for microbiome and the supernatant reserved for metabolomics. All samples were frozen at −80°C and shipped to University of North Carolina (UNC) on dry ice. AREST subjects with CF had chest CTs performed using standard AREST CF protocols, with lobe-specific scores generated using a modified CF-CT scoring system (*2*, *63*). Anti-staphylococcal prophylaxis (amoxicillin–clavulanic acid) was routinely prescribed during the first 2 years of life to children with CF at the PMHC. Parental informed consent was obtained of all study participants, with ethical approval by the UNC Institutional Review Board (protocol number 12-1538) and the PMHC (registration number 1762/EP).

Total mucin concentration, IHC staining for flake mucins, IHC image analyses, and SEM

Total mucin concentrations were measured on unprocessed BALF samples by Sepharose 2B column/refractometry–based quantitation as previously described (*60*). Unprocessed BALF (20 μl) was applied to glass microscopy slides and cytocentrifuged (StatSpin CytoFuge 2, Beckman Coulter Inc.). Slides were fixed with neutral buffered formalin (10 volume %), washed with Dulbecco's phosphate-buffered saline (DPBS), and blocked with bovine serum albumin (3 weight % in DPBS) for 1 hour at room temperature. MUC5AC and MUC5B were immunohistochemically stained (0.4 and 0.2 μg/ml with mouse anti-MUC5AC and rabbit anti-MUC5B antibodies, respectively), slides were washed with DPBS three times (10 min), exposed to secondary antibodies [Alexa Fluor 488 and 594 (1 μg/ml) anti-rabbit and anti-mouse, respectively] and DAPI (5 μg/ml) to stain for DNA for 1 hour at 25°C, and then washed with DPBS (10 min) and mounted with FluorSave (Calbiochem). Note that at all times, the specimens were maintained in a hydrated environment. Quantitative measurements of stain intensity from confocal images were obtained with an Olympus FV1000 (Olympus, Hamilton, Bermuda) using a 10× objective and uniform settings. SEM was performed on 60-μl unprocessed BALF, raw or exposed to treatments, deposited onto poly-D-lysine (12-mm coverslips), allowed to sediment (2 hours at room temperature), fixed, dehydrated, critically point-dried, mounted on planchets, sputtered with 8-nm gold palladium alloy, and viewed on a Supra 25 scanning electron microscope (Zeiss).

Mucin granularity (RMS roughness) and rheology

Three-channel red-green-blue images of stained BALF samples taken at ×60 magnification were converted into grayscale images and then decomposed into a two-dimensional wave number (ν) representation via a two-dimensional Fourier transform. Power spectral densities of the transformed images were calculated, and the values were summed over both dimensions, following Elson and Bennett (*17*), yielding the RMS of image granularity, or dominant wave number. Granularity was calculated as the RMS wave number after application of a high-pass filter to remove features larger than 1 μm ($\nu = 106\ m^{-1}$). Each population value represents the average granularity of one to three images per patient sample. The results of the 1-μm threshold are presented to exclude nuclei and whole flakes while including the granular features observed in CF images. The 1-μm filter is also relevant in light of previous reports stating that the sizes of compacted granular complexes of secreted mucins are on the order of ~0.5 to 1 μm in diameter (*64*). All RMS wave number calculations and image processing were performed and automated via a custom-written MATLAB (The MathWorks, 2017) script. Passive microbead rheology was performed as previously described (*60*) on unprocessed BALF samples gently centrifuged (2000*g* × 30 s) to recover the insoluble flakes and allowed to equilibrate with 1 μm of polyethylene glycol (PEG)–coated beads via overnight incubation. A

bimodal distribution was noted and fitted using a two Gaussian mixture model via the MATLAB function fitgmdist, which identified a sharp peak (mean $\eta^* = 0.89 \times 10^{-3}$ Pa·s) centered about the viscosity of water and a second broad peak (mean $\eta^* = 0.0593$ Pa·s) corresponding to the range of 1.5 to 4.5% solids by weight HBE mucus (*60*).

Metabolomics

Untargeted metabolomic profiling was performed on 60 BALF supernatants representing the two lavage samples from 23 CF individual subjects (7 subjects were studied at more than one study visit). Samples were chosen to be representative of the disease severity of the full study population, with 23.3% of samples from lobes with bronchiectasis on chest CT and 53.3% from lobes with BWT. Samples were analyzed by Metabolon Inc. using three independent platforms (ultrahigh-performance liquid chromatography/tandem mass spectrometry for acidic and basic metabolites, as well as gas chromatography/mass spectrometry) as previously described (*65*). Metabolites were identified by automated comparison of ion features to a reference library. Values below limits of detection were imputed from the minimum detectable value.

Inflammation and microbiology analyses

Inflammatory markers, including cell counts/differential, neutrophil elastase, and IL-8, were measured from a separate lavage of the RML per standard AREST CF protocols. Bacterial cultures were performed in the PMHC clinical microbiology laboratory, with pathogenic infection defined as growth of $\geq 10^3$ organisms/ml of any specific organism other than mixed oral flora, with a threshold of $\geq 10^4$ organisms/ml used for some analyses as specified in the text. (*20*).

Microbiome and qPCR analyses

BALF samples were centrifuged at 18,000*g* for 5 min at 4°C, and excess supernatant was removed to yield a final sample of ~200 µl. Bacteria within samples were chemically lysed per manufacturer's instructions for the Roche MagNA Pure Compact System Automated DNA Extraction (Roche Diagnostics). First, samples were resuspended and incubated in an enzyme cocktail (lysozyme and lysostaphin), followed by a second incubation with bacteria lysis buffer and proteinase K. The samples were then inactivated for pathogenicity at 95°C for 10 min, vortexing intermittently, and allowed to cool to room temperature before loading onto the extraction system. The V3 and V4 region of the bacterial 16*S* ribosomal RNA (rRNA) gene was amplified from about 100 ng of template DNA in a 50-µl reaction with Phusion Hot Start II DNA Polymerase (Thermo Fisher Scientific) using modified universal 338F and 806R primers (98°C for 30 s, 25 cycles of 98°C for 10 s, 52°C for 30 s, 72°C for 20 s, followed by 72°C for 5 min) (*66*). Amplicons were cleaned with Axygen AxyPrep Mag PCR Clean-up Kit (Axygen Scientific) according to the manufacturer's instructions using a 1:1 ratio. Bead-cleaned products were tagged with Illumina barcodes and Nextera adapters (98°C for 30 s, 20 cycles of 98°C for 10 s, 63°C for 30 s, 72°C for 30 s, followed by 72°C for 5 min), purified again with Axygen beads as above, and visualized on a 1% agarose gel for appropriate fragment size (about 600 base pairs). Products were quantified with Quant-iT PicoGreen dsDNA Assay Kit (Thermo Fisher Scientific), pooled in equimolar amounts (up to 20 µl of product) and sequenced at the UNC High-Throughput Sequencing Facility on an Illumina MiSeq using a V3, paired-end, 600-cycle kit (Illumina Inc.). Raw sequence data were deposited in the European Nucleotide Archive (study accession number PRJEB22216). Paired ends were joined using FastQ-Join (default parameters) within QIIME (version 1.8.0) (*67*). Sequence data were demultiplexed with a custom AWK script designed to remove inline primer sequences and retain 16*S* ribosomal DNA sequences with greater than 85% of bases exceeding a *Q* score of 28. Operational taxonomic unit (OTUs) were determined via the open reference OTU picking workflow in QIIME, pick_open_reference_otus.py, where GreenGenes 13.8 served as a reference for both OTUs and taxonomy (*68*). Chimeras were detected and removed from the dataset using ChimeraSlayer within QIIME. After removing OTUs that were taxonomically unassigned (Kingdom: Unassigned), sequences were rarefied to 10,000 sequences per sample for all other downstream analyses.

Quantification of bacterial 16*S* rRNA gene copies was performed using QuantStudio 6 Flex Real-Time PCR System (Thermo Fisher Scientific) used as previously described (*69*), targeting the V1 and V2 16*S* rRNA gene with primers purchased from Integrated DNA Technologies (V1_forward: AGAGTTTGATCCTGGCTCAG, V2_reverse: CTGCTGCCTYCCGTA, probe:

FAM-TA + ACA + CATG+CA + AGTC + GA-BHQ1).

Microbead rheology

The passive diffusion of 1-µm PEG-coated beads incubated with unprocessed BALF samples was tracked and used to calculate complex viscosities (η^*) from individual and ensemble beads as previously described (*60*).

Whole-sample imaging

Beads entrapped in mucus flakes were imaged via yellow-green fluorescence on an Olympus IX70 inverted light microscope using an automated stage. Individual 2048 pixel × 2048 pixel (210 × 210 µm) fields were imaged via phase contrast and yellow-green fluorescence with 10-ms exposures, and the imaging process was repeated using preprogrammed motion (cellSens Dimension software, Olympus, 2017) for the entire slide. The image series was stitched together, and metrics regarding flake size and abundance were obtained using a custom written MATLAB program (The MathWorks, 2017). The program outlined flake regions based on a user-determined threshold that was modified to ensure optimal identification of visible flakes.

Mucus flake treatment

BALF samples were spun at 2000*g* for 30 s to accumulate mucus at the bottom of the microcentrifuge tube, with 180 µl of sample, including the pellet, transferred to a new microcentrifuge tube using a Gilson positive pressure pipette and mixed. For each administration, 27 µl of the sample was aliquoted to a fresh tube with 3 µl of drug treatment (10 mM DTT, 3/30 mM NAC, or 2.5/25 mM P2062) or DNAse (0.3 U/µl) for 1 hour at 37°C before analysis by IHC, whole-sample imaging, SEM, or microbead rheology. P2062 activity was compared to NAC using an artificial S-S substance DNTB [5,5′-dithiobis-(2-nitrobenzoic acid] (*70*) and via Western blots of CF sputum using rabbit anti-MUC5B (H300, Santa Cruz Biotechnology) antibodies as previously described (*71*). IRDye secondary antibody fluorescence was detected with a LI-COR Odyssey Infrared Imaging System.

Sheep studies

TMV measurements were made in adult naïve or HNE (Elastin Products Company) pretreated female sheep as previously described (*24*). P2062 was administered via aerosolization at a dose of 50 mg/kg. Vehicle was PBS.

Statistical analysis

Mucus analyses were performed per lobe and compared with lobe-specific microbiology, inflammatory markers, and CT data. Comparisons among groups (CF versus non-CF) used mixed-effects models with random intercepts to account for repeated visits, adjusted for lobe (samples from two lobes available per subject), gender, and age. Simple correlations used linear regressions. Multivariate analyses used general estimating equation models fitted for each variable with binomial family, logit link, and robust SEs and were adjusted as above. Treatment studies were analyzed using repeated-measures analysis of variance (ANOVA). Data not normally distributed were log-transformed before analysis. Statistical analyses were performed using GraphPad Prism v5.0 and Stata (version 13.0; StataCorp). All data are presented as means ± SD.

SUPPLEMENTARY MATERIALS

www.sciencetranslationalmedicine.org/cgi/content/full/11/486/eaav3488/DC1

Fig. S1. Mucin flakes in CF.
Fig. S2. Molecular microbiology in CF samples.
Fig. S3. CF microbiology and antibiotic use.
Fig. S4. Microrheologic effects of treatment.
Fig. S5. P2062.
Fig. S6. Disease pathogenesis in normal and early CF lung.
Table S1. Diagnoses in non-CF disease control populations.
Table S2. Bacterial infection by conventional culture in AREST CF and non-CF disease control populations as a function of bacterial density.
Table S3. Multivariate analyses for BALF mucin parameters.
Table S4. Correlation of mucins, MUC5B and MUC5AC to markers of inflammation and metabolomic markers of airway environment in CF BALF.
Table S5. Multivariate analyses of mucins versus BALF metabolomic and inflammatory markers.
Table S6. BALF markers in CF-NSD versus non-CF controls.
Data file S1. Raw data (provided as separate Excel file).

REFERENCES AND NOTES

1. P. B. Davis, Cystic fibrosis since 1938. *Am. J. Respir. Crit. Care Med.* **173**, 475–482 (2006).
2. L. S. Mott, J. Park, C. P. Murray, C. L. Gangell, N. H. de Klerk, P. J. Robinson, C. F. Robertson, S. C. Ranganathan, P. D. Sly, S. M. Stick; AREST CF, Progression of early structural lung disease in young children with cystic fibrosis assessed using CT. *Thorax* **67**, 509–516 (2012).
3. P. D. Sly, S. Brennan, C. Gangell, N. de Klerk, C. Murray, L. Mott, S. M. Stick, P. J. Robinson, C. F. Robertson, S. C. Ranganathan; Australian Respiratory Early Surveillance Team for Cystic Fibrosis (AREST-CF), Lung disease at diagnosis in infants with cystic fibrosis detected by newborn screening. *Am. J. Respir. Crit. Care Med.* **180**, 146–152 (2009).
4. C. Ehre, C. Ridley, D. J. Thornton, Cystic fibrosis: An inherited disease affecting mucin-producing organs. *Int. J. Biochem. Cell Biol.* **52**, 136–145 (2014).
5. S. Farber, H. Shwachman, C. L. Maddock, Pancreatic function and disease in early life. I. Pancreatic enzyme activity and the celiac syndrome. *J. Clin. Invest.* **22**, 827–838 (1943).
6. A. G. Henderson, C. Ehre, B. Button, L. H. Abdullah, L.-H. Cai, M. W. Leigh, G. C. DeMaria, H. Matsui, S. H. Donaldson, C. W. Davis, J. K. Sheehan, R. C. Boucher, M. Kesimer, Cystic fibrosis airway secretions exhibit mucin hyperconcentration and increased osmotic pressure. *J. Clin. Invest.* **124**, 3047–3060 (2014).
7. B. Button, L.-H. Cai, C. Ehre, M. Kesimer, D. B. Hill, J. K. Sheehan, R. C. Boucher, M. Rubinstein, A periciliary brush promotes the lung health by separating the mucus layer from airway epithelia. *Science* **337**, 937–941 (2012).
8. M. Mall, B. R. Grubb, J. R. Harkema, W. K. O'Neal, R. C. Boucher, Increased airway epithelial Na^+ absorption produces cystic fibrosis-like lung disease in mice. *Nat. Med.* **10**, 487–493 (2004).
9. J. J. Smith, S. M. Travis, E. P. Greenberg, M. J. Welsh, Cystic fibrosis airway epithelia fail to kill bacteria because of abnormal airway surface fluid. *Cell* **85**, 229–236 (1996).
10. D. A. Stoltz, D. K. Meyerholz, A. A. Pezzulo, S. Ramachandran, M. P. Rogan, G. J. Davis, R. A. Hanfland, C. Wohlford-Lenane, C. L. Dohrn, J. A. Bartlett, G. A. Nelson Jr., E. H. Chang, P. J. Taft, P. S. Ludwig, M. Estin, E. E. Hornick, J. L. Launspach, M. Samuel, T. Rokhlina, P. H. Karp, L. S. Ostedgaard, A. Uc, T. D. Starner, A. R. Horswill, K. A. Brogden, R. S. Prather, S. S. Richter, J. Shilyansky, P. B. McCray Jr., J. Zabner, M. J. Welsh, Cystic fibrosis pigs develop lung disease and exhibit defective bacterial eradication at birth. *Sci. Transl. Med.* **2**, 29ra31 (2010).
11. N. S. Joo, H.-J. Cho, M. Khansaheb, J. J. Wine, Hyposecretion of fluid from tracheal submucosal glands of CFTR-deficient pigs. *J. Clin. Invest.* **120**, 3161–3166 (2010).
12. C. Sorio, A. Montresor, M. Bolomini-Vittori, S. Caldrer, B. Rossi, S. Dusi, S. Angiari, J. E. Johansson, M. Vezzalini, T. Leal, E. Calcaterra, B. M. Assael, P. Melotti, C. Laudanna, Mutations of cystic fibrosis transmembrane conductance regulator gene cause a monocyte-selective adhesion deficiency. *Am. J. Respir. Crit. Care Med.* **193**, 1123–1133 (2016).
13. P. M. Quinton, Cystic fibrosis: Impaired bicarbonate secretion and mucoviscidosis. *Lancet* **372**, 415–417 (2008).
14. A. Heeckeren, R. Walenga, M. W. Konstan, T. Bonfield, P. B. Davis, T. Ferkol, Excessive inflammatory response of cystic fibrosis mice to bronchopulmonary infection with Pseudomonas aeruginosa. *J. Clin. Invest.* **100**, 2810–2815 (1997).
15. B. H. Rosen, T. I. A. Evans, S. R. Moll, J. S. Gray, B. Liang, X. Sun, Y. Zhang, C. W. Jensen-Cody, A. M. Swatek, W. Zhou, N. He, P. G. Rotti, S. R. Tyler, N. W. Keiser, P. J. Anderson, L. Brooks, Y. Li, R. M. Pope, M. Rajput, E. A. Hoffman, K. Wang, J. K. Harris, K. R. Parekh, K. N. Gibson-Corley, J. F. Engelhardt, Infection is not required for Mucoinflammatory lung disease in CFTR-knockout ferrets. *Am. J. Respir. Crit. Care Med.* **197**, 1308–1318 (2018).
16. N. W. Keiser, S. E. Birket, I. A. Evans, S. R. Tyler, A. K. Crooke, X. Sun, W. Zhou, J. R. Nellis, E. K. Stroebele, K. K. Chu, G. J. Tearney, M. J. Stevens, J. K. Harris, S. M. Rowe, J. F. Engelhardt, Defective innate immunity and hyperinflammation in newborn cystic fibrosis transmembrane conductance regulator-knockout ferret lungs. *Am. J. Respir. Cell Mol. Biol.* **52**, 683–694 (2015).
17. J. M. Elson, J. M. Bennett, Calculation of the power spectral density from surface profile data. *Appl. Optics* **34**, 201–208 (1995).
18. C. R. Esther Jr., L. Turkovic, T. Rosenow, M. S. Muhlebach, R. C. Boucher, S. Ranganathan, S. M. Stick; AREST CF, Metabolomic biomarkers predictive of early structural lung disease in cystic fibrosis. *Eur. Respir. J.* **48**, 1612–1621 (2016).
19. C. R. Esther Jr., R. D. Coakley, A. G. Henderson, Y. H. Zhou, F. A. Wright, R. C. Boucher, Metabolomic evaluation of neutrophilic airway inflammation in cystic fibrosis. *Chest* **148**, 507–515 (2015).
20. K. A. Ramsey, S. Ranganathan, J. Park, B. Skoric, A.-M. Adams, S. J. Simpson, R. M. Robins-Browne, P. J. Franklin, N. H. de Klerk, P. D. Sly, S. M. Stick, G. L. Hall; AREST CF, Early respiratory infection is associated with reduced spirometry in children with cystic fibrosis. *Am. J. Respir. Crit. Care Med.* **190**, 1111–1116 (2014).
21. S. Yuan, M. Hollinger, M. E. Lachowicz-Scroggins, S. C. Kerr, E. M. Dunican, B. M. Daniel, S. Ghosh, S. C. Erzurum, B. Willard, S. L. Hazen, X. Huang, S. D. Carrington, S. Oscarson, J. V. Fahy, Oxidation increases mucin polymer cross-links to stiffen airway mucus gels. *Sci. Transl. Med.* **7**, 276ra227 (2015).
22. M. Djabourov, K. Bouchemal, in *Disordered Pharmaceutical Materials,* M. Descamps, Ed. (Wiley-VCH, Weinheim, Germany, 2016), pp. 241–282.
23. K. D. Held, J. E. Biaglow, Mechanisms for the oxygen radical-mediated toxicity of various thiol-containing compounds in cultured mammalian cells. *Radiat. Res.* **139**, 15–23 (1994).
24. J. R. Sabater, T. A. Lee, W. M. Abraham, Comparative effects of salmeterol, albuterol, and ipratropium on normal and impaired mucociliary function in sheep. *Chest* **128**, 3743–3749 (2005).
25. S. Gehrig, J. Duerr, M. Weitnauer, C. J. Wagner, S. Y. Graeber, J. Schatterny, S. Hirtz, A. Belaaouaj, A. H. Dalpke, C. Schultz, M. A. Mall, Lack of neutrophil elastase reduces inflammation, mucus hypersecretion, and emphysema, but not mucus obstruction, in mice with cystic fibrosis-like lung disease. *Am. J. Respir. Crit. Care Med.* **189**, 1082–1092 (2014).
26. R. A. Caldwell, R. C. Boucher, M. J. Stutts, Neutrophil elastase activates near-silent epithelial Na^+ channels and increases airway epithelial Na^+ transport. *Am. J. Physiol. Lung Cell. Mol. Physiol.* **288**, L813–L819 (2005).
27. R. C. Boucher, Airway surface dehydration in cystic fibrosis: Pathogenesis and therapy. *Annu. Rev. Med.* **58**, 157–170 (2007).
28. M. Kesimer, A. M. Makhov, J. D. Griffith, P. Verdugo, J. K. Sheehan, Unpacking a gel-forming mucin: A view of MUC5B organization after granular release. *Am. J. Physiol. Lung Cell. Mol. Physiol.* **298**, L15–L22 (2010).
29. A. A. Hyman, C. A. Weber, F. Jülicher, Liquid-liquid phase separation in biology. *Annu. Rev. Cell Dev. Biol.* **30**, 39–58 (2014).
30. D. L. Simel, J. P. Mastin, P. C. Pratt, C. L. Wisseman, J. D. Shelburne, A. Spock, P. Ingram, Scanning electron microscopic study of the airways in normal children and in patients with cystic fibrosis and other lung diseases. *Pediatr. Pathol.* **2**, 47–64 (2009).
31. L. S. Ostedgaard, T. O. Moninger, J. McMenimen, N. M. Sawin, C. P. Parker, I. M. Thornell, L. S. Powers, N. D. Gansemer, D. C. Bouzek, D. P. Cook, D. K. Meyerholz, M. H. Abou Alaiwa, D. A. Stoltz, M. J. Welsh, Gel-forming mucins form distinct morphologic structures in airways. *Proc. Natl. Acad. Sci. U.S.A.* **114**, 6842–6847 (2017).
32. A. Ermund, L. N. Meiss, A. M. Rodriguez-Pineiro, A. Bähr, H. E. Nilsson, S. Trillo-Muyo, C. Ridley, D. J. Thornton, J. J. Wine, H. Hebert, N. Klymiuk, G. C. Hansson, The normal trachea is cleaned by MUC5B mucin bundles from the submucosal glands coated with the MUC5AC mucin. *Biochem. Biophys. Res. Commun.* **492**, 331–337 (2017).

33. A. Ermund, L. N. Meiss, B. Dolan, A. Bähr, N. Klymiuk, G. C. Hansson, The mucus bundles responsible for airway cleaning are retained in cystic fibrosis and by cholinergic stimulation. *Eur. Respir. J.* **52**, 1800457 (2018).
34. H. A. W. M. Tiddens, S. H. Donaldson, M. Rosenfeld, P. D. Paré, Cystic fibrosis lung disease starts in the small airways: Can we treat it more effectively? *Pediatr. Pulmonol.* **45**, 107–117 (2010).
35. V. S. Shah, D. K. Meyerholz, X. X. Tang, L. Reznikov, M. Abou Alaiwa, S. E. Ernst, P. H. Karp, C. L. Wohlford-Lenane, K. P. Heilmann, M. R. Leidinger, P. D. Allen, J. Zabner, P. B. McCray Jr., L. S. Ostedgaard, D. A. Stoltz, C. O. Randak, M. J. Welsh, Airway acidification initiates host defense abnormalities in cystic fibrosis mice. *Science* **351**, 503–507 (2016).
36. A. Schultz, R. Puvvadi, S. M. Borisov, N. C. Shaw, I. Klimant, L. J. Berry, S. T. Montgomery, T. Nguyen, S. M. Kreda, A. Kicic, P. B. Noble, B. Button, S. M. Stick, Airway surface liquid pH is not acidic in children with cystic fibrosis. *Nat. Commun.* **8**, 1409 (2017).
37. J. E. Pittman, K. M. Wylie, K. Akers, G. A. Storch, J. Hatch, J. Quante, K. B. Frayman, N. Clarke, M. Davis, S. M. Stick, G. L. Hall, G. Montgomery, S. Ranganathan, S. D. Davis, T. W. Ferkol; Australian Respiratory Early Surveillance Team for Cystic Fibrosis, Association of antibiotics, airway microbiome, and inflammation in infants with cystic fibrosis. *Ann. Am. Thorac. Soc.* **14**, 1548–1555 (2017).
38. E. T. Zemanick, B. D. Wagner, C. E. Robertson, R. C. Ahrens, J. F. Chmiel, J. P. Clancy, R. L. Gibson, W. T. Harris, G. Kurland, T. A. Laguna, S. A. McColley, K. McCoy, G. Retsch-Bogart, K. T. Sobush, P. L. Zeitlin, M. J. Stevens, F. J. Accurso, S. D. Sagel, J. K. Harris, Airway microbiota across age and disease spectrum in cystic fibrosis. *Eur. Respir. J.* **50**, 1700832 (2017).
39. M. S. Muhlebach, B. T. Zorn, C. R. Esther, J. E. Hatch, C. P. Murray, L. Turkovic, S. C. Ranganathan, R. C. Boucher, S. M. Stick, M. C. Wolfgang, Initial acquisition and succession of the cystic fibrosis lung microbiome is associated with disease progression in infants and preschool children. *PLOS Pathog.* **14**, e1006798 (2018).
40. M. M. Tunney, T. R. Field, T. F. Moriarty, S. Patrick, G. Doering, M. S. Muhlebach, M. C. Wolfgang, R. Boucher, D. F. Gilpin, A. McDowell, J. S. Elborn, Detection of anaerobic bacteria in high numbers in sputum from patients with cystic fibrosis. *Am. J. Respir. Crit. Care Med.* **177**, 995–1001 (2008).
41. E. S. Cowley, S. H. Kopf, A. LaRiviere, W. Ziebis, D. K. Newman, Pediatric cystic fibrosis sputum can be chemically dynamic, anoxic, and extremely reduced due to hydrogen sulfide formation. *MBio* **6**, e00767 (2015).
42. B. Mirkovic, M. A. Murray, G. M. Lavelle, K. Molloy, A. A. Azim, C. Gunaratnam, F. Healy, D. Slattery, P. McNally, J. Hatch, M. Wolfgang, M. M. Tunney, M. S. Muhlebach, R. Devery, C. M. Greene, N. G. McElvaney, The role of short-chain fatty acids, produced by anaerobic bacteria, in the cystic fibrosis airway. *Am. J. Respir. Crit. Care Med.* **192**, 1314–1324 (2015).
43. J. M. Flynn, D. Niccum, J. M. Dunitz, R. C. Hunter, Evidence and role for bacterial mucin degradation in cystic fibrosis airway disease. *PLOS Pathog.* **12**, e1005846 (2016).
44. S. D. Sagel, R. L. Gibson, J. Emerson, S. McNamara, J. L. Burns, J. S. Wagener, B. W. Ramsey; Inhaled Tobramycin in Young Children Study Group, Cystic Fibrosis Foundation Therapeutics Development Network, Impact of *Pseudomonas* and *Staphylococcus* infection on inflammation and clinical status in young children with cystic fibrosis. *J. Pediatr.* **154**, 183–188.e3 (2009).
45. D. Willner, M. R. Haynes, M. Furlan, N. Hanson, B. Kirby, Y. W. Lim, P. B. Rainey, R. Schmieder, M. Youle, D. Conrad, F. Rohwer, Case studies of the spatial heterogeneity of DNA viruses in the cystic fibrosis lung. *Am. J. Respir. Cell Mol. Biol.* **46**, 127–131 (2012).
46. F. J. Reen, D. F. Woods, M. J. Mooij, M. N. Chróinín, D. Mullane, L. Zhou, J. Quille, D. Fitzpatrick, J. D. Glennon, G. P. McGlacken, C. Adams, F. O'Gara, Aspirated bile: A major host trigger modulating respiratory pathogen colonisation in cystic fibrosis patients. *Eur. J. Clin. Microbiol. Infect. Dis.* **33**, 1763–1771 (2014).
47. D. Armstrong, K. Grimwood, J. B. Carlin, R. Carzino, J. Hull, A. Olinsky, P. D. Phelan, Severe viral respiratory infections in infants with cystic fibrosis. *Pediatr. Pulmonol.* **26**, 371–379 (1998).
48. P. McNally, E. Ervine, M. D. Shields, B. D. Dimitrov, B. El Nazir, C. C. Taggart, C. M. Greene, N. G. McElvaney, P. Greally, High concentrations of pepsin in bronchoalveolar lavage fluid from children with cystic fibrosis are associated with high interleukin-8 concentrations. *Thorax* **66**, 140–143 (2011).
49. O. W. Williams, A. Sharafkhaneh, V. Kim, B. F. Dickey, C. M. Evans, Airway mucus: From production to secretion. *Am. J. Respir. Cell Mol. Biol.* **34**, 527–536 (2006).
50. A. Livraghi-Butrico, B. R. Grubb, K. J. Wilkinson, A. S. Volmer, K. A. Burns, C. M. Evans, W. K. O'Neal, R. C. Boucher, Contribution of mucus concentration and secreted mucins Muc5ac and Muc5b to the pathogenesis of muco-obstructive lung disease. *Mucosal Immunol.* **10**, 395–407 (2017).
51. B. Fritzsching, Z. Zhou-Suckow, J. B. Trojanek, S. C. Schubert, J. Schatterny, S. Hirtz, R. Agrawal, T. Muley, N. Kahn, C. Sticht, N. Gunkel, T. Welte, S. H. Randell, F. Länger, P. Schnabel, F. J. F. Herth, M. A. Mall, Hypoxic epithelial necrosis triggers neutrophilic inflammation via IL-1 receptor signaling in cystic fibrosis lung disease. *Am. J. Respir. Crit. Care Med.* **191**, 902–913 (2015).
52. S. T. Montgomery, A. S. Dittrich, L. W. Garratt, L. Turkovic, D. L. Frey, S. M. Stick, M. A. Mall, A. Kicic; AREST CF, Interleukin-1 is associated with inflammation and structural lung disease in young children with cystic fibrosis. *J. Cyst. Fibros.* **17**, 715–722 (2018).
53. J. J. Tyson, K. C. Chen, B. Novak, Sniffers, buzzers, toggles and blinkers: Dynamics of regulatory and signaling pathways in the cell. *Curr. Opin. Cell Biol.* **15**, 221–231 (2003).
54. X. Luan, G. Belev, J. S. Tam, S. Jagadeeshan, N. Hassan, P. Gioino, N. Grishchenko, Y. Huang, J. L. Carmalt, T. Duke, T. Jones, B. Monson, M. Burmester, T. Simovich, O. Yilmaz, V. A. Campanucci, T. E. Machen, L. D. Chapman, J. P. Ianowski, Cystic fibrosis swine fail to secrete airway surface liquid in response to inhalation of pathogens. *Nat. Commun.* **8**, 786 (2017).
55. T. L. Bonfield, C. A. Hodges, C. U. Cotton, M. L. Drumm, Absence of the cystic fibrosis transmembrane regulator (*Cftr*) from myeloid-derived cells slows resolution of inflammation and infection. *J. Leukoc. Biol.* **92**, 1111–1122 (2012).
56. M. W. Konstan, C. L. Hoppel, B. L. Chai, P. B. Davis, Ibuprofen in children with cystic fibrosis: Pharmacokinetics and adverse effects. *J. Pediatr.* **118**, 956–964 (1991).
57. F. Ratjen, L. Saiman, N. Mayer-Hamblett, L. C. Lands, M. Kloster, V. Thompson, P. Emmett, B. Marshall, F. Accurso, S. Sagel, M. Anstead, Effect of azithromycin on systemic markers of inflammation in patients with cystic fibrosis uninfected with Pseudomonas aeruginosa. *Chest* **142**, 1259–1266 (2012).
58. R. G. Iannitti, V. Napolioni, V. Oikonomou, A. de Luca, C. Galosi, M. Pariano, C. Massi-Benedetti, M. Borghi, M. Puccetti, V. Lucidi, C. Colombo, E. Fiscarelli, C. Lass-Flörl, F. Majo, L. Cariani, M. Russo, L. Porcaro, G. Ricciotti, H. Ellemunter, L. Ratclif, F. M. de Benedictis, V. N. Talesa, C. A. Dinarello, F. L. van de Veerdonk, L. Romani, IL-1 receptor antagonist ameliorates inflammasome-dependent inflammation in murine and human cystic fibrosis. *Nat. Commun.* **7**, 10791 (2016).
59. T. J. Torphy, J. Allen, A. M. Cantin, M. W. Konstan, F. J. Accurso, E. Joseloff, F. A. Ratjen, J. F. Chmiel; Antiinflammatory Therapy Working Group, Considerations for the conduct of clinical trials with Antiinflammatory agents in cystic fibrosis. A Cystic Fibrosis Foundation workshop report. *Ann. Am. Thorac. Soc.* **12**, 1398–1406 (2015).
60. D. B. Hill, P. A. Vasquez, J. Mellnik, S. A. McKinley, A. Vose, F. Mu, A. G. Henderson, S. H. Donaldson, N. E. Alexis, R. C. Boucher, M. G. Forest, A biophysical basis for mucus solids concentration as a candidate biomarker for airways disease. *PLOS ONE* **9**, e87681 (2014).
61. M. Rosenfeld, F. Ratjen, L. Brumback, S. Daniel, R. Rowbotham, S. McNamara, R. Johnson, R. Kronmal, S. D. Davis; ISIS Study Group, Inhaled hypertonic saline in infants and children younger than 6 years with cystic fibrosis: The ISIS randomized controlled trial. *JAMA* **307**, 2269–2277 (2012).
62. L. H. Abdullah, R. Coakley, M. J. Webster, Y. Zhu, R. Tarran, G. Radicioni, M. Kesimer, R. C. Boucher, C. W. Davis, C. M. P. Ribeiro, Mucin production and hydration responses to mucopurulent materials in normal versus cystic fibrosis airway epithelia. *Am. J. Respir. Crit. Care Med.* **197**, 481–491 (2018).
63. A. S. Brody, H. A. W. M. Tiddens, R. G. Castile, H. O. Coxson, P. A. de Jong, J. Goldin, W. Huda, F. R. Long, M. McNitt-Gray, M. Rock, T. E. Robinson, S. D. Sagel, CT Scanning in Cystic Fibrosis Special Interest Group, Computed tomography in the evaluation of cystic fibrosis lung disease. *Am. J. Respir. Crit. Care Med.* **172**, 1246–1252 (2005).
64. L. H. Abdullah, J. R. Evans, T. T. Wang, A. A. Ford, A. M. Makhov, K. Nguyen, R. D. Coakley, J. D. Griffith, C. W. Davis, S. T. Ballard, M. Kesimer, Defective postsecretory maturation of MUC5B mucin in cystic fibrosis airways. *JCI Insight* **2**, e89752 (2017).
65. A. M. Evans, C. D. DeHaven, T. Barrett, M. Mitchell, E. Milgram, Integrated, nontargeted ultrahigh performance liquid chromatography/electrospray ionization tandem mass spectrometry platform for the identification and relative quantification of the small-molecule complement of biological systems. *Anal. Chem.* **81**, 6656–6667 (2009).
66. D. S. Lundberg, S. Yourstone, P. Mieczkowski, C. D. Jones, J. L. Dangl, Practical innovations for high-throughput amplicon sequencing. *Nat. Methods* **10**, 999–1002 (2013).
67. J. G. Caporaso, J. Kuczynski, J. Stombaugh, K. Bittinger, F. D. Bushman, E. K. Costello, N. Fierer, A. G. Peña, J. K. Goodrich, J. I. Gordon, G. A. Huttley, S. T. Kelley, D. Knights, J. E. Koenig, R. E. Ley, C. A. Lozupone, D. McDonald, B. D. Muegge, M. Pirrung, J. Reeder, J. R. Sevinsky, P. J. Turnbaugh, W. A. Walters, J. Widmann, T. Yatsunenko, J. Zaneveld, R. Knight, QIIME allows analysis of high-throughput community sequencing data. *Nat. Methods* **7**, 335–336 (2010).
68. T. Z. DeSantis, P. Hugenholtz, N. Larsen, M. Rojas, E. L. Brodie, K. Keller, T. Huber, D. Dalevi, P. Hu, G. L. Andersen, Greengenes, a chimera-checked 16S rRNA gene database and workbench compatible with ARB. *Appl. Environ. Microbiol.* **72**, 5069–5072 (2006).
69. C. M. Bassis, J. R. Erb-Downward, R. P. Dickson, C. M. Freeman, T. M. Schmidt, V. B. Young, J. M. Beck, J. L. Curtis, G. B. Huffnagle, Analysis of the upper respiratory tract microbiotas as the source of the lung and gastric microbiotas in healthy individuals. *MBio* **6**, e00037 (2015).
70. P. W. Riddles, R. L. Blakeley, B. Zerner, Ellman's reagent: 5,5′-dithiobis(2-nitrobenzoic acid)—A reexamination. *Anal. Biochem.* **94**, 75–81 (1979).
71. K. A. Ramsey, Z. L. Rushton, C. Ehre, Mucin agarose gel electrophoresis: Western blotting for high-molecular-weight glycoproteins. *J. Vis. Exp.* 10.3791/54153 (2016).
72. S. M. P. J. Prevaes, W. A. A. de Steenhuijsen Piters, K. M. de Winter-de Groot, H. M. Janssens, G. A. Tramper-Stranders, M. L. J. N. Chu, H. A. Tiddens, M. van Westreenen, C. K. van der Ent, E. A. M. Sanders, D. Bogaert, Concordance between upper and lower airway microbiota in infants with cystic fibrosis. *Eur. Respir. J.* **49**, 1602235 (2017).

Acknowledgments: We thank M. Rubinstein for many helpful discussions. We acknowledge the contributions of present and past members of the AREST CF. **Funding:** C.R.E., L.T., M.S.M., and S.M.S. were supported by NIH/NHLBI R01-HL116228. C.R.E. was also supported by NC TraCS 50KR51009, NIH/NIEHS P30-ES10126, and NIH/NHLBI K23-HL089708. L.T. and S.M.S. were supported by NHMRC GNT1000896. S.M.S. was supported by a NHMRC Practitioner Fellowship GNT 111840. R.C.B. was supported by NIH/NHLBI UH3-HL123645, P01-HL108808, P30-DK065988, P01-HL110873, P50-HL107168, and R01-HL136961. M.G.F., D.B.H., and I.S. were supported by NSF-NIGMS DMS-1462992. K.A.R. and C.E. were supported by Cystic Fibrosis Foundation RAMSEY16I0 and a NHMRC Early Career Fellowship (APP1088389) and EHRE 16XX0 and EHRE07XX0. **Author contributions:** C.R.E. and M.S.M. obtained funding, performed and designed experiments, interpreted results, and wrote the manuscript. C.E., D.B.H., M.K., K.A.R., M.R.M., and I.C.G. performed mucin measurements and IHC. M.C.W. and B.Z. performed microbiome experiments. M.G.F. and I.S. assisted interpretation and results of microbead rheology data. C.B.M. and M.F.D. performed SEM experiments. W.R.T. and D.V. developed P2062 and helped design experiments. J.R.S. developed the sheep model and ran sheep studies. L.T. performed biostatistical analyses. S.R. and S.M.S. co-established the AREST CF platforms and sampling methods. S.R. obtained funding and reviewed and edited results and the manuscript. S.M.S. and R.C.B. co-contributed as senior authors, obtained funding, interpreted results, and edited the manuscript. **Competing interests:** W.R.T. and D.V. are employees of Parion Sciences, which is developing mucolytic reducing agents similar to those used in this manuscript. R.C.B. has financial interests in Parion Sciences. The authors declare that they have no other competing interests. **Data and materials availability:** Microbiome sequencing data were deposited into the European Nucleotide Archive (study accession number PRJEB22216). All the data for this study are present in the main text or in the Supplementary Materials.

Submitted 12 September 2018
Accepted 10 March 2019
Published 3 April 2019
10.1126/scitranslmed.aav3488

Citation: C. R. Esther Jr., M. S. Muhlebach, C. Ehre, D. B. Hill, M. C. Wolfgang, M. Kesimer, K. A. Ramsey, M. R. Markovetz, I. C. Garbarine, M. G. Forest, I. Seim, B. Zorn, C. B. Morrison, M. F. Delion, W. R. Thelin, D. Villalon, J. R. Sabater, L. Turkovic, S. Ranganathan, S. M. Stick, R. C. Boucher, Mucus accumulation in the lungs precedes structural changes and infection in children with cystic fibrosis. *Sci. Transl. Med.* **11**, eaav3488 (2019).